Ionization potentials of porphyrins and phthalocyanines. A comparative benchmark study of fast improvements of Koopman's Theorem

Dennis P. Piet,[a] David Danovich,[b] Han Zuilhof *[a] and Ernst J. R. Sudhölter *[a]

[a] *Laboratory of Organic Chemistry, Department of Biomolecular Sciences, Wageningen University and Research Center, Dreijenplein 8, 6703 HB Wageningen, The Netherlands*
[b] *Department of Chemistry and Lise Meitner Minerva Center for Computational Quantum Chemistry, Hebrew University, Givat-Ram Campus, 91904 Jerusalem, Israel*

The vertical ionization potentials (IP's) of a variety of free-base and zinc porphyrins and free-base and zinc phthalocyanine, including *all* those for which experimental ultraviolet photoelectron spectral (UPS) data are presently known, are computed using six semiempirical molecular orbital methods. Koopman's Theorem (KT), second order outer valence Green's function methods with a large number of active orbitals (OVGF), and explicit computation of the relative energies of neutral species and vertically ionized radical cations (ΔSCF IP) are used in combination with both PM3 and AM1 parameterizations, and the results are compared to experimental data. On average, both the OVGF and ΔSCF IP approximations reproduce the first vertical IP's, as determined by UPS, far more accurately than KT at minimal extra computational costs. Over the full set of available experimental data, the average error for the lowest IP with both OVGF and ΔSCF IP is only *ca.* 40% of that of KT (AM1 data, AM1 being generally more accurate than PM3). Inclusion of higher order terms in the OVGF treatment (third order truncation or full expression of the self-energy part) does not affect the computed IP's significantly, but inclusion of a large number of active orbitals in the OVGF technique is shown to be essential for this class of molecules. In agreement with the experimental data, zinc porphyrins and zinc phthalocyanines are computed to be better electron donors than their free-base analogues. Conformational differences of the peripheral substituents have no significant effects on the valence IP's.

Introduction

Large aromatic systems, such as porphyrins (P's) and phthalocyanines (Pc's, see Fig. 1) are of substantial interest for the development of electro-optical devices,[1] ion complexation[2] and biological redox reactions.[3] To be able to apply these materials as sensitizing dyes in organic solar cells,[4] which form a central part of our research, more detailed knowledge is required of those properties that are relevant in photo-induced electron transfer processes, *e.g.*, the oxidation potential of the dye molecule. Since the ionization potential (IP) is a dominant factor in the determination of oxidation potentials (E_{ox} ~ IP + solvation terms), trends in the oxidation potentials are reproduced in the ionization potentials if there is a near-constant difference between the vertical and adiabatic IP's along a series of compounds of interest. As this has been shown to be the case for the series of tetrapyrrolic compounds of interest,[5] computation of the vertical IP's thus yields a fast selection method for molecules that might be synthesized for use in organic solar cells.

It is known that chemical modification of these dyes *via* peripheral substitution of the aromatic macrocycle with electron-donating and -withdrawing substituents, as well as linear and angular annelation of the ring significantly affects the energy levels of the molecular orbitals.[6] One of our research objectives is the selective positioning of the highest occupied molecular orbital (HOMO) level of porphyrins, porphyrazines and phthalocyanines by variations in the peripheral substitution pattern and the central ligand. The first electronically excited state (S_1) of tetrapyrroles can be estimated from a combination of electrochemical data (reduction potentials) and absorption and luminescence data. It has been shown that variations in the substitution pattern that cause the first IP to decrease will for many substituents also cause a corresponding rise in the excited state energy (relative to the vacuum level).[6a] Since the driving force ΔG for photo-induced electron transfer is determined by the relative energy of the $\Delta E(S_1 - S_0)$ and the oxidation level E_{ox} of the donor, accurate knowledge of these parameters is
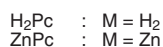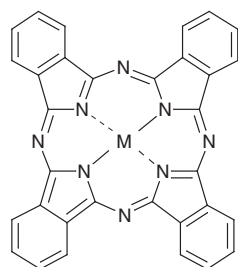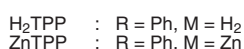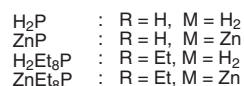

H₂P   : R = H, M = H₂
ZnP   : R = H, M = Zn
H₂Et₈P : R = Et, M = H₂
ZnEt₈P : R = Et, M = Zn

H₂TPP   : R = Ph, M = H₂
ZnTPP   : R = Ph, M = Zn

H₂Pc   : M = H₂
ZnPc   : M = Zn
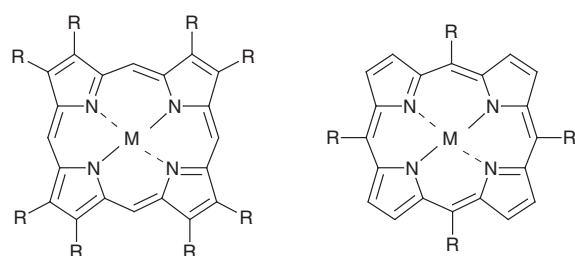
Fig. 1 Structures of compounds studied in this work.

Orbital Relaxation   Electron Correlation

—— ·· —— ———— ----- ——   rad.cat.

total
energy |

——— ---- ———   ———— ·· ——   neutral
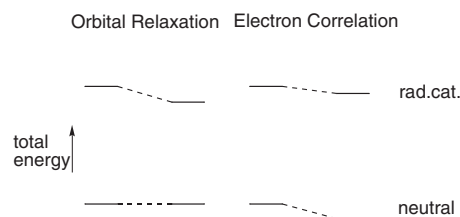
Fig. 2 Effect of orbital relaxation and electron correlation on the total electronic energy of the radical cation with respect to that of the neutral precursor (left of dashed lines: neglect of effect; right of dashed line: taking account of effect).

instrumental for the systematic construction of organic solar cells.

Computations of ionization potentials (IP's) of molecules are traditionally performed using Koopman's Theorem (KT).[7] According to KT the IP's are the sign-reversed orbital energies: IP $\approx -E_{\text{HOMO}}$. This approach uses a frozen-orbital approximation, in which the orbitals of the final ionized state are assumed to be identical to those of the neutral state. It does thus neglect two oppositely directed energy contributions that play a significant and sometimes dominant role in the electronic structure of the radical cation (Fig. 2).[8] First, Koopman's theorem neglects the orbital relaxation after the ionization step. Due to the removal of the electron, the coefficients of the molecular orbitals in the molecular ion will tend to change with respect to the values of the neutral precursor. By neglecting this orbital relaxation, the energy of the computed radical cation will be too high, as well as the computed IP. In KT, however, this error (Err$^{\text{relax}}$) is frequently compensated for by an oppositely directed error due to electron correlation effects (Err$^{\text{corr}}$). These correlation effects are smaller in the radical cation than in the neutral molecule, due to the loss of an electron. Taking appropriate account of electron correlation will therefore lead to a smaller energy lowering of the radical cation than of the neutral species. Neglect of the electron correlation would thus yield a computed IP which is too low (Fig. 2). Fortunately, in many cases, these errors are approximately the same size (Err$^{\text{relax}} \approx$ Err$^{\text{corr}}$) which makes KT a crude but useful model.[9]

The applicability of KT changes for those molecules in which this cancellation of errors fails, or in which contributions from non-Koopman's electronic configurations can not be neglected in the description of the final ionized state. This is, in fact, frequently the case, even with relatively small electronic structures such as benzene and pyridine, in which the application of KT yields errors up to 2 eV.[10] This means that KT can really only be used for an approximation of IP in those cases in which the effects of both orbital relaxation and electron correlation errors are known or reliably estimated. In many cases this is not *a priori* possible, which makes KT quantitatively unreliable. As the degree of the resulting deviation from the experimental values can usually not be accurately estimated based on the Hartree–Fock (HF) molecular orbital energies alone, more quantitatively reliable models are highly desirable.

In the development of large tetrapyrrolic systems like peripherally substituted porphyrins and phthalocyanines for their potential use in dye-sensitized organic solar cells, large series of compounds need to be evaluated with regard to their electron-donating properties.[11] Routine prediction of the IP's of low-symmetry materials by the use of *ab initio* HF or density functional theory (DFT) calculations is not feasible due to the prohibitively large number of integrals and corresponding CPU-time. DFT calculations on the core orbital and the valence orbital energies of porphyrins and porphyrazines have been reported,[12] which are generally in good agreement with experimentally obtained vertical IP values derived from X-ray and ultraviolet photoelectron spectroscopy (XPS and UPS, respectively). However, even taking into account the molecular symmetry of these molecules, such calculations are still very

time-consuming and frequently not routinely accessible for the calculation of the IP's of large series of large molecules, specifically those of C_1 symmetry. It is therefore clear that at present fast and reliable semiempirical improvements over KT are still highly desirable. In this paper, two alternatives are tested by comparison of the computational results with all the presently available UPS data on free-base and zinc porphyrins and free-base and zinc phthalocyanines.

The outer valence Green's functions approach (OVGF), originally developed by the Cederbaum group,[13] allows for a quantitative estimation of both electron correlation and orbital relaxation effects. It was recently shown that OVGF can be efficiently coupled to semiempirical molecular orbital methods (like AM1 and PM3) to form a fast and reliable method for calculating ionization potentials that is significantly more accurate than KT for a wide range of materials.[14,15] Specifically the improvement for nitrogen-containing heterocycles is noteworthy.[14b] The theory of the OVGF method as well as the explicit formulae are given elsewhere,[16] and will thus only be described briefly here. The one particle Green's function method is one of the most valid approaches to the calculations of the photoelectron spectrum.[17] In this method, Hartree–Fock solutions (orbital energies and corresponding integrals) are used as the zeroth-order approximation, and many-body perturbation theory is used in order to obtain straightforward equations which provide, in a single calculation, the desired ionization potentials with correlation and relaxation effects accounted for. A detailed account of the approximations that are convenient for the numerical realization of this method has been published.[16]

One of the attractive features of the OVGF approach is that only computation of the neutral species is required, *i.e.* no explicit computation of the vertically ionized radical cation is required. Since the latter might be troublesome, due to the open electron shell and concomitant computational difficulties, alternative approaches such as OVGF demand attention, specifically as it is fast even compared to the semiempirical minimization process. The alternative for OVGF thus consists of explicit computation of the energies of both the neutral compound and the resulting radical cation after vertical ionization. This procedure has been labeled ΔSCF IP, but can be used as easily for post-SCF methods. This method comprises two computational actions, but the second step (here: single point computation of the energy of the vertically ionized radical cation) is very fast compared to the geometry optimization of the neutral system. Both OVGF and ΔSCF IP therefore provide fast alternatives to KT, but the question, of course, is: how accurate are these approaches?

This work presents the results of a comparative benchmark study on the performance of six methods to predict the vertical IP's of several peripherally substituted porphyrins and phthalocyanines. KT, OVGF and ΔSCF IP were to this aim applied with the AM1[18] and PM3[19] parameterizations using the MOPAC 93 program.[20] The computational results are compared with (to the best of our knowledge) *all* presently reported vertical IP data, as obtained using UPS for tetrapyrrole compounds, and as such constitute a critical test of the methods under study.

Computational details

Geometry optimizations were performed using the MOPAC 93 program[20] within C_1 symmetry with the PM3 and AM1 parameterizations implemented in there, using a Z-matrix or cartesian coordinates with the keywords: VECTORS AM1/PM3 GEO-OK PRECISE GNORM=0.1. The symmetry labels of the MO's of species with internal symmetry are frequently not assigned within MOPAC 93, and were in those cases obtained by performing the corresponding semiempirical single point calculation at the optimized structures within the

Table 1 Vertical ionization potentials of H_2P as calculated by KT, OVGF and ΔSCF, and experimental UPS data (in eV; see text)

| IP's | Symm.[a] | PM3 | | | | | AM1 | | | | | UPS peaks[b] |
		KT	OVGF (2)	(3)	(Full)	ΔSCF	KT	OVGF (2)	(3)	(Full)	ΔSCF	
IP_1	b_{3u}	7.68	7.29	7.30	7.30	7.24	7.80	7.37	7.38	7.38	7.41	6.9
IP_2	a_u	8.09	7.73	7.75	7.74		7.79	7.46	7.50	7.49		7.2
IP_3	b_{1g}	9.59	9.06	9.00	9.02		9.71	9.09	9.02	9.04		8.8
IP_4	b_{3u}	9.65	9.03	8.99	9.01		9.79	9.22	9.18	9.19		9.1
Δ[c]		0.8	0.3	0.3	0.3		0.8	0.3	0.3	0.3		

[a] The orbital labeling refers to the symmetry of the corresponding MO. [b] See ref. 23. [c] Mean deviation between the calculated and the experimental values for the first four IP's.

Table 2 Dependence of the OVGF-calculated vertical IP (in eV) of free-base porphyrin H_2P on the number of active orbitals

| IP's | Symm.[a] | PM3 | | | | | AM1 | | | | | UPS peaks[b] |
		20–20[c]	30–30	40–40	50–50	57–53	20–20	30–30	40–40	50–50	57–53	
IP_1	b_{3u}	7.29	7.17	7.13	7.09	7.07	7.37	7.23	7.18	7.13	7.11	6.9
IP_2	a_u	7.73	7.65	7.60	7.58	7.56	7.46	7.33	7.28	7.25	7.23	7.2
IP_3	b_{1g}	9.06	8.90	8.82	8.77	8.75	9.09	8.94	8.86	8.80	8.78	8.8
IP_4	b_{3u}	9.03	8.90	8.90	8.86	8.85	9.22	9.07	9.07	8.94	8.90	9.1
Δ[d]		0.3	0.3	0.2	0.2	0.2	0.3	0.2	0.1	0.1	0.1	

[a] The orbital labeling refers to the symmetry of the corresponding MO. [b] See ref. 23. [c] 20–20 denotes an active orbital window of the highest 20 occupied orbitals, and the lowest 20 unoccupied orbitals. [d] Mean deviation between the calculated and the experimental values for the first four IP's.

GAUSSIAN94 suite of programs.[21] The outer valence Green's functions approach was used *via* an adaptation of MOPAC 93 which includes dynamic memory allocation to allow its application to large molecules. Second order, third order and full expressions for the self-energy part were applied in the computations of the IP's using the keyword GREENF(IT23=0). The number of active orbitals (default: 20 occupied and 20 virtual orbitals) was increased with the keyword GREENF(NOCC= n,NVIR=m), in which n is the number of occupied orbitals, and m the number of unoccupied orbitals in the neutral molecule. Neutral species were computed using restricted Hartree–Fock computations, and Dewar's half-electron procedure was used to describe the radical cation (MOPAC keyword: OPEN(1,1)).[22] Reported computation times were obtained with a Silicon Graphics O2 machine with one R10000 processor and 192 MB RAM. With enough RAM similar results can be obtained on either G3 Powermacs or Pentium II/III machines.

Results and discussion

Method dependence of IP computation: effect of OVGF truncation

The IP's of the free-base porphyrin (H_2P) were calculated using the OVGF approach within the AM1 and PM3 approximation (denoted as OVGF(AM1) and OVGF(PM3), respectively), with the self-energy part including different orders of perturbation corrections. The full expression for the self-energy part is required in *ab initio* calculations to obtain quantitatively reliable results. Great computational advantages are obtained with semiempirical methods, especially since these also have been shown in several cases to require only second-order perturbation corrections.[14,15] The effect of truncation at the second order on the lowest four IP's (IP_1–IP_4) was investigated first using the default number of 40 active orbitals (20 highest occupied MO's and the 20 lowest unoccupied MO's; short: 20 HOMO's–20 LUMO's). This is relevant, since the calculation time using the full expression is approximately 30 minutes on a small workstation, while with truncation at the second-order level the computation time only takes several seconds.

The results in Table 1 clearly show that for both the PM3 and

the AM1 parameters the computed IP's are only slightly affected when the third-order and the full expression for the self-energy part are used. The first IP of H_2P was calculated to be 7.29 eV and 7.37 eV, truncated at the second-order, for OVGF(PM3) and OVGF(AM1), respectively. This only changes slightly, and never more than 0.07 eV, for IP_1 and IP_2 when a third-order truncation or the full expression for the self-energy part are applied. This range of higher order effects (all differences ≤ 0.1 eV, without systematic improvements at higher levels) was also found for other porphyrins and phthalocyanines. Due to the lack of systematic improvements in combination with the small size of the effect compared to the uncertainty limits for nearly all reported experimental data, all further calculations discussed in this paper were truncated at the second-order perturbation correction level.

Method dependence of IP computation: AM1 *vs.* PM3

The relative merits[23] of the PM3 and AM1 parameterization for the computation of IP's were evaluated over the whole series of species under study. From the results in Tables 1–8 (which will be discussed in more detail later) it can be seen that, on an overall basis, AM1 produces results that are more in line with observed experimental data, especially in the case of metallated tetrapyrroles. Certain exceptions were found, but as a general method for fast accurate computations of the IP's of tetrapyrrolic systems, AM1 is preferable to PM3. Since we consider this as an empirical finding, we will for reasons of clarity restrict the discussion in the text to the AM1 results. The relevant PM3 data are also presented in Tables 1–8 to enable the reader to compare these directly, but will only be discussed in special cases.

Method dependence of IP computation: effect of number of active orbitals

The dependence of the calculated IP's on the number of active orbitals taken into the OVGF calculations is presented in Table 2 and Fig. 3. As can be seen from Table 2, an increase of the number of active orbitals systematically improves the results of the OVGF calculations on H_2P. An increase from the default value of 20 HOMO's–20 LUMO's) to the full set of 57
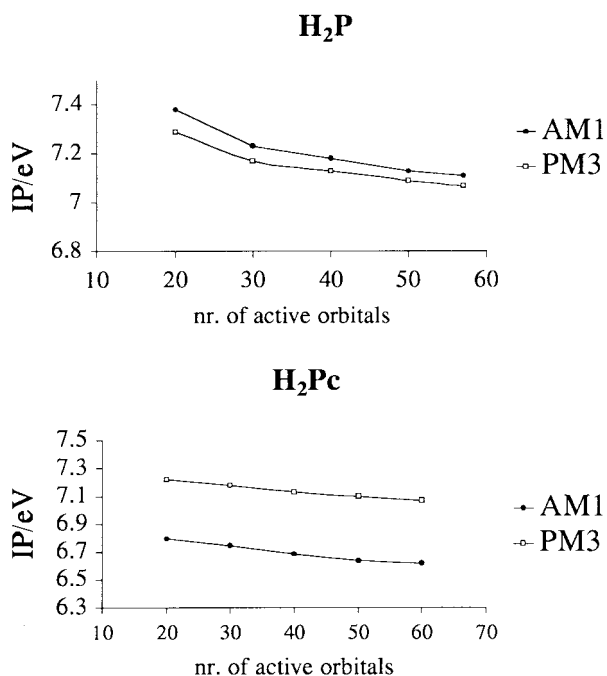
H₂P

H₂Pc

Fig. 3 Effect of the number of active orbitals on the OVGF-calculated IP's of H₂P (top) and H₂Pc (bottom).

HOMO's–53 LUMO's decreases the theoretical experimental disagreement by 0.2 eV for OVGF(PM3) and 0.1 eV for OVGF(AM1) over the first four IP's. Unfortunately, such increases of the active orbital window also lead to increases in CPU-time and computer memory demands. For a relatively small macrocycle like H₂P, inclusion of all active orbitals poses no practical problems. However, for substituted porphyrins and phthalocyanines the substantially larger number of potentially active orbitals (>200) changes this picture. In order to find an optimum between the size of the active orbital window and the accuracy of the calculated IP's, the orbital window of free-base phthalocyanine H₂Pc is increased stepwise to a maximum set of 60 HOMO's–60 LUMO's. As can be seen from Fig. 3, an active orbital window of 60 HOMO's–60 LUMO's gives excellent results in an acceptable timeframe. Therefore, an active orbital window of 60 HOMO's–60 LUMO's is used for all OVGF calculations.

Ionization potentials of porphyrins

Porphyrin (H₂P). For H₂P, IP₁ and IP₂ have been determined by UPS[24] to be 6.9 eV and 7.2 eV. This near-degeneracy of the b_{3u} and a_u HOMO's is predicted in Gouterman's four orbital theory,[25] according to which the two lowest IP's should be well separated from all higher IP's in the porphyrin system. KT(AM1) predicts IP₁ and IP₂ to be nearly degenerate at 7.79 eV and 7.80 eV, respectively, while OVGF(AM1) places the first two IP's at 7.11 eV and 7.23 eV, in excellent agreement with the experimental data. The third IP is with OVGF(AM1) even quantitatively reproduced ($IP_{exp} = 8.8$ eV; $IP_{calc} = 8.78$ eV), while the fourth IP is also in good agreement with experiment ($IP_{exp} = 9.1$ eV; $IP_{calc} = 8.90$ eV). The ΔSCF IP(AM1) IP of H₂P is calculated to be 7.41 eV, which is 0.3 eV less accurate than OVGF(AM1) but still significantly better than KT.

Free-base and zinc octaethylporphyrin (H₂Et₈P and ZnEt₈P). In the case of free-base octaethylporphyrin (H₂Et₈P) the presence of eight ethyl substituents will result in a large number of different conformations. In order to determine the effect of different geometries of the octaethyl substituents on the valence IP's, four different conformations of H₂Et₈P, as shown in Fig. 4, were minimized and their lowest IP's calculated: all-*trans* (AT),
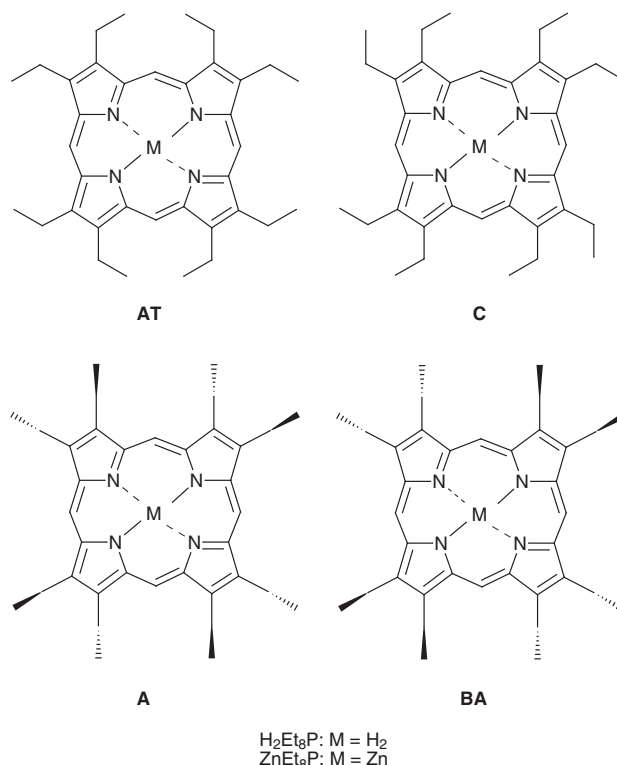

H₂Et₈P: M = H₂
ZnEt₈P: M = Zn

Fig. 4 Four characteristic geometries of octaethylporphyrin; all-*trans* (AT), clockwise (C), alternating (A) and bi-alternating (BA).

clockwise (C), alternating (A) and bi-alternating (BA). Upon minimization both the AT and C conformers converge to the BA structure, the most stable conformation of H₂Et₈P. The A conformer is also stable, and its heat of formation (ΔH_f) is only 0.2 kcal mol⁻¹ above ΔH_f of the BA conformer. In contrast, constrained optimization of AT and C (all C and N atoms in the molecule fixed within one plane) leads to structures that are, respectively, 30 and 40 kcal mol⁻¹ higher than that of the (BA) structure. The IP's of the planar AT and C conformers did not deviate significantly from those of the BA conformer (<0.1 eV), but due to their chemical instability will not be discussed further. The values for IP₁–IP₄ of the A and BA conformers of H₂Et₈P as calculated using KT, OVGF and ΔSCF IP are compiled in Table 3.

It is clear from Table 3 that different geometries of the peripheral ethyl substituents have no significant effect on the four highest MO's: all differences are within a 0.05 eV margin. This is of interest for our solar cell work, as in such devices ordering of these dyes *via* the liquid crystalline hexagonal discotic phase is crucial for optimal energy and charge transport. In such a phase the π-moieties of the dyes are well ordered in large stacks, but much less is known about the ordering and rotational freedom of the alkyl substituent. The implication of the observed invariance of the IP on the orientation of the substituent is that conformational freedom of the side-chain has no detrimental effects on the electron-donating properties of the dye, which is as desired.

Both KT(PM3) and KT(AM1) place the first IP at 7.55 eV, over 1 eV higher than the experimental value of H₂Et₈P of 6.39 eV.[26] The first IP as calculated by OVGF(AM1) of 6.99 eV improves 0.56 eV on KT, while with ΔSCF IP(AM1) a nearly identical value (7.00 eV) is computed. It should be noted that IP₁ and IP₂ as calculated by OVGF(AM1) are energetically virtually identical, as the prediction of the second IP is significantly more accurate than the first. This gap itself is computed to be more in line with experiment when OVGF(PM3) is used, but the constituting IP's are both no improvement over OVGF(AM1). As in the case of H₂P, the two lowest IP's, as calculated by KT and OVGF, are energetically well separated

Table 3 Vertical ionization potentials of H_2Et_8P as calculated by KT, OVGF and ΔSCF, and experimental UPS data (in eV; see text)

Geometry	IP	AM1			PM3			UPS peaks[a]
		KT	OVGF	ΔSCF	KT	OVGF	ΔSCF	
BA	IP_1	7.54	6.99	7.00	7.55	7.00	7.05	6.39
	IP_2	7.64	6.99		7.87	7.36		6.83
	IP_3	9.17	8.37		9.13	8.39		7.55
	IP_4	9.19	8.38		9.25	8.52		7.80
A	IP_1	7.55	6.99	7.00	7.57	7.02	7.06	
	IP_2	7.64	7.00		7.85	7.34		
	IP_3	9.16	8.36		9.09	8.36		
	IP_4	9.19	8.37		9.24	8.52		
	Δ^b	1.24	0.54		1.27	0.64		

[a] See ref. 26. [b] Mean deviation between the calculated and the experimental values for the first four IP's.

Table 4 Vertical ionization potentials of $ZnEt_8P$ as calculated by KT, OVGF and ΔSCF, and experimental UPS data (in eV; see text)

Geometry	IP	AM1			PM3			UPS peaks[a]
		KT	OVGF	ΔACF	KT	OVGF	ΔSCF	
BA	IP_1	7.17	6.67	6.71	7.54	7.05	7.13	6.29
	IP_2	7.54	6.93		7.63	7.22		6.72
	IP_3	8.91	7.87		8.95	8.01		7.71
	IP_4	9.35	8.33		9.22	8.29		8.04
A	IP_1	7.17	6.66	6.71	7.54	7.05	7.13	
	IP_2	7.54	6.93		7.64	7.22		
	IP_3	8.90	7.86		8.92	7.99		
	IP_4	9.34	8.33		9.21	8.28		
	Δ^b	1.05	0.26		1.11	0.42		

[a] See reference 26. [b] Mean deviation between the calculated and the experimental values for the first four IP's.

from all other IP's, which is in accordance with Gouterman's four orbital model.

Local density function (LDF) calculations have been used by Ghosh *et al.* to study peripheral substituent effects on valence IP's of free base porphyrins with electron-donating and -withdrawing groups,[12d,27] but the effect of different spatial conformations of the peripheral groups on the valence IP's was not reported. LDF calculations on H_2Me_8P yield for the lowest IP a value of 6.64 eV,[27] which is close to the experimental value of H_2Et_8P; no LDF value for H_2Et_8P has as yet been reported.

The half-wave potential of H_2Et_8P in solution is known to exhibit variations up to 1 eV with a change in the central metal atom.[28] However, UPS measurements on metallo–octaethylporphyrins have clearly shown that changes in the central metal atom are of little influence on the valence IP's. Compared to H_2Et_8P, a maximum increase in the first IP of approximately 0.3 eV was observed when the core protons are exchanged for either an iron(II) or cobalt(II), while insertion of zinc(II) only raises the first IP by ~ 0.1 eV.[28] The effect of a zinc atom in the central cavity is investigated for two reasons: 1) incorporation of zinc leads to an increase in the electron-donating properties,[29] and 2) parameterization of zinc is available in both the semiempirical PM3 and AM1 methods, which allows for a more systematic comparison between the two methods. Table 4 summarizes the IP data of the KT, OVGF and ΔSCF IP calculations for $ZnEt_8P$. The effect of the different conformations of the peripheral ethyl substituents was studied in the same way as for H_2Et_8P, *i.e.* the same four characteristic geometry types (AT, C, A, and BA) were minimized for $ZnEt_8P$ and IP_1–IP_4 determined.

As is the case with H_2Et_8P, conformational differences of the β-ethyl substituents exert little effect on the experimental IP's of $ZnEt_8P$ (<0.05 eV). The effect of metal insertion into the porphyrin cavity on the semiempirical calculations is somewhat larger, especially when the AM1 minimization procedure is used. As can be seen from Table 4, the IP-decreasing effect of Zn-substitution is reproduced by OVGF(AM1), albeit some-

what too strongly (ΔIP_{calc} = 0.33 eV; ΔIP_{exp} = 0.10 eV). The OVGF(AM1)-calculated first IP of PEt_8Zn of 6.66 eV is 0.05 eV more accurate than ΔSCF IP (experimental value: 6.29 eV[26]). KT(AM1) predicts the first IP of $ZnEt_8P$ to be 7.17 eV, 0.38 eV higher than the value of H_2Et_8P, and the overestimation of the experimental IP is still 0.88 eV. This case is a typical one in which AM1 performs better than PM3. KT(PM3), OVFG(PM3) and ΔSCF IP(PM3) predict the first IP of $ZnEt_8P$ to be 7.50 eV, 7.01 eV and 7.13 eV, which in all cases is 0.3–0.4 eV less accurate than their AM1 counterparts. The KT(PM3) value differs only 0.05 eV from its free base counterpart, *i.e.* reproduces the small effect of Zn-substitution, but deviates more than 1.2 eV from the experimental value of 6.29 eV.[25] The effect of zinc insertion is, however, not consistently predicted with PM3: with ΔSCF IP(AM1) the calculated first IP decrease with Zn insertion is from 7.00 to 6.71 eV, while ΔSCF IP(PM3) predicts an increase in the first IP of 0.09 eV.

***meso*-Tetraphenylporphyrin (H_2TPP).** It has been recognized that *meso*-substituents exert stronger effects on the ionization potentials than the same substituents placed on the β-positions of porphyrins.[27,30] As is the case with the β-ethyl substituents of the ethylporphyrins, rotation of the four phenyl groups of H_2TPP results in a large number of different conformations. Gassman *et al.* have computed that the valence level orbital energies of the D_{2h} and C_{2v} conformers of H_2TPP are within a 0.05 eV margin.[12] A number of porphyrins possess a ruffled or saddle-shaped chromophore instead of a planar aromatic unit.[28b,31] Due to this ruffling, the porphyrin is oxidized more easily whereas reduction is insensitive to the distortion as was observed by electrochemical measurements.[31b] The influence of this puckering on the IP's of H_2TPP was investigated by single point calculations of two different experimental crystal structures, a triclinic and a tetragonal one with the two semiempirical methods.[33] In the tetragonal H_2TPP structure, the phenyl groups are tilted approximately 60° with respect to the saddle-shaped porphyrin, while in the triclinic structure the

Table 5 Vertical ionization potentials of monoclinic TPPH$_2$ as calculated with KT, OVGF and ΔSCF, and experimental UPS data (in eV; see text)

Geometry	IP	AM1			PM3			UPS peaks[a]
		KT	OVGF	ΔSCF	KT	OVGF	ΔSCF	
Tetragonal	IP$_1$	7.12	6.64	6.61	7.02	6.68	6.57	6.39
	IP$_2$	7.50	7.03		7.76	7.29		6.72
	IP$_3$	9.44	8.26		9.45	8.36		7.71
	IP$_4$	9.55	8.34		9.56	8.51		8.86
	Δ[b]	0.98	0.41		1.03	0.47		
Triclinic	IP$_1$	7.19	6.74	6.73	7.09	6.76	6.67	
	IP$_2$	7.53	7.11		7.78	7.33		
	IP$_3$	9.60	8.44		9.60	8.49		
	IP$_4$	9.66	8.69		9.65	8.75		
	Δ[b]	1.06	0.41		1.11	0.47		

[a] See ref. 32. [b] Mean deviation between the calculated and the experimental values for the first four IP's.

Table 6 Vertical ionization potentials of monoclinic TPPZn as calculated with KT, OVGF and ΔSCF, and experimental UPS data (in eV; see text)
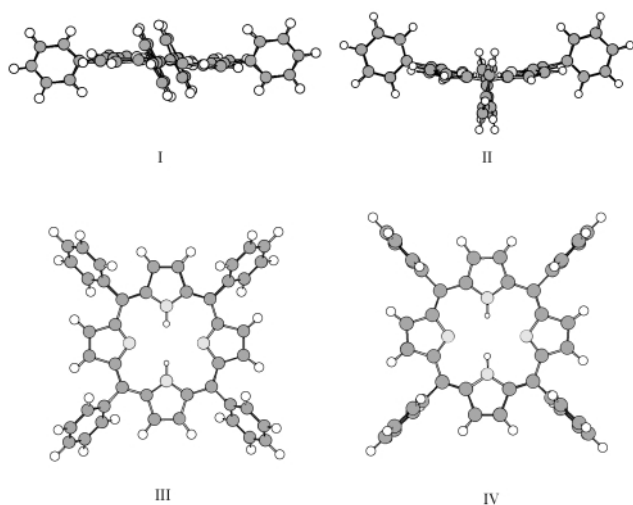
IP	AM1			PM3			UPS peaks[a]
	KT	OVGF	ΔSCF	KT	OVGF	ΔSCF	
IP$_1$	7.44	6.97	6.99	7.54	7.21	7.14	6.42
IP$_2$	7.47	7.05		7.84	7.34		6.62
IP$_3$	9.74	8.60		9.55	8.46		7.76
IP$_4$	9.82	9.23		9.67	8.57		8.73
Δ[d]	1.25	0.58		1.27	0.59		

[a] See ref. 32. [b] Mean deviation between the calculated and the experimental values for the first four IP's.

Fig. 5 Different geometries of H$_2$TPP; triclinic side-view (I), tetragonal side-view (II), triclinic top-view (III), tetragonal top-view (IV).

macrocycle is relatively planar. However, two opposing phenyl rings are invertedly twisted along the *z*-axis by 5° (Fig. 5). In Table 5, IP$_1$–IP$_4$ values of both H$_2$TPP crystal structures are compiled together with their experimental values.[30]

As can be seen from Table 5, there are no major differences between the valence level energies of triclinic and tetragonal H$_2$TPP. Therefore, puckering of the porphyrin macrocycle does not lead to a significant change of the IP according to these semiempirical computations. KT(AM1) calculates the first IP of tetragonal H$_2$TPP to be 7.12 eV, which yields a discrepancy of 0.73 eV with the experimental value of 6.39 eV. The OVGF(AM1) procedure computes IP$_1$ at 6.64 eV, which is 0.48 eV better than KT(AM1) and differs only 0.25 eV from the experimental value. ΔSCF IP(AM1) calculates IP$_1$ = 6.61 eV for tetragonal H$_2$TPP and 6.73 eV for triclinic H$_2$TPP, again in excellent agreement with the experimental data (deviations ∼ 0.2–0.3 eV). The second IP is also computed in good agreement with experiment: 6.72 eV and 7.03 eV, for respectively the

experimental value and that computed for the tetragonal structure. The third and fourth IP are anticipated in a region of the UPS spectrum that is dominated by ionizations arising from the phenyl substituents. For instance, a simple aromatic compound like toluene displays its first IP at 8.83 eV.[34] Apparently, the increased electronic correlation involved in ionizations arising from a combination of the chromophore and the phenyl substituents yields with all methods, including OVGF(AM1), an increased discrepancy between the calculated and the experimentally observed third and fourth IP of both tetragonal and triclinic H$_2$TPP. This suggests a limitation of the applicability of this technique to the lower IP's of *meso*-tetraarylporphyrins. Gouterman's four orbital theory holds for the experimental H$_2$TPP structures when calculated by the AM1 method: the first two IP's are well separated from the two higher IP's. A difference of *ca*. 0.4 eV between IP$_1$ and IP$_2$ is computed with both the KT and OVGF approximations, in good agreement with the experimental difference of 0.33 eV. When computed with PM3, the difference between the first two IP's amounts to 0.7 eV for both experimental structures.

Zinc *meso*-tetraphenylporphyrin (ZnTPP). The vast majority of ZnTPP crystallographic data is presented with either one or two axial ligands. It is known that axial ligation has a substantial influence on the redox properties, both in solution[35] and in a film,[36] and on the photovoltaic properties.[37] Only one data set for ZnTPP without axial ligands has been published.[38] In this monoclinic structure, two opposing phenyl groups are tilted approximately 76° with respect to the porphyrin plane, while the other two opposing phenyl groups are tilted approximately 73°. KT, OVGF and ΔSCF IP data on this geometry of ZnTPP are presented in Table 6.

KT(AM1) calculates IP$_1$ = 7.44 eV, a difference of 1.02 eV with the experimental value of 6.42 eV.[33] Both the OVGF(AM1) and ΔSCF IP(AM1) computed first IP of 6.97 eV and 6.99 eV, respectively, agree significantly better with experiment, though the deviations are still >0.5 eV. The two lowest IP's, as calculated by KT and OVGF, are energetically well separated from all other IP's and nearly degenerate, which is in accordance with Gouterman's four orbital model. Comparison

Table 7 Vertical ionization potentials of monoclinic PcH$_2$ as calculated with KT, OVGF and ΔSCF, and experimental UPS data (in eV; see text)

Symm.[a]	AM1			PM3			UPS peaks[b]
	KT	OVGF	ΔSCF	KT	OVGF	ΔSCF	
a$_u$	7.15	6.62	6.57	7.63	7.07	7.08	6.41
b$_{3u}$	9.24	8.37		9.00	8.16		8.75
b$_{1g}$	9.50	8.51		9.29	8.57		
b$_{3u}$	9.65	8.85		9.61	8.98		
Δ[c]	0.62	0.30		0.74	0.62		

[a] The orbital labeling referes to the symmetry of the corresponding MO. [b] See ref. 41. [c] Mean deviation between the calculated and the experimental values for the first four IP's.

Table 8 Vertical ionization potentials of monoclinic PcZn as calculated with KT, OVGF and ΔSCF. and experimental UPS data (in eV; see text)

Symm.[a]	AM1			PM3			UPS peaks[b]
	KT	OVGF	ΔSCF	KT	OVGF	ΔSCF	
a$_{1u}$	6.87	6.46	6.39	7.37	6.86	6.90	6.37
a$_{2u}$	9.17	8.23		9.06	8.27		8.50
e$_g$	9.44	8.44		9.30	8.46		8.96
e$_g$	9.57	8.73		9.56	8.85		9.34
Δ[c]	0.47	0.37		0.53	0.43		

[a] The orbital labeling refers to the symmetry of the corresponding MO. [b] See ref. 41. [c] Mean deviation between the calculated and the experimental values for the first four IP's.

of the data of H$_2$TPP and ZnTPP in Tables 5 and 6 shows that insertion of a zinc into the central cavity of the porphyrin hardly affects the IP's, which is in contrast with the effects of metallation of H$_2$Et$_8$P. The computed differences between H$_2$TPP and ZnTPP might well be caused to a substantial degree by differences in the crystal structures involved: H$_2$TPP structures are somewhat (axially) deformed by ring-puckering and tilting of the C_{ipso}–C_{para} line in the phenyl rings out of the plane of the macrocycle, while monoclinic ZnTPP possesses a planar framework with the phenyl rings placed only in a tilted position towards the macrocycle. Single-point computations on these deformed structures may lead to an increase of the computed IP's.

Free-base phthalocyanine and zinc phthalocyanine (H$_2$Pc and ZnPc). Phthalocyanines (Pc's) have received considerable attention in the study of energy and electron transfer processes. The spontaneous cofacial arrangement of Pc's with long peripheral alkyl and alkoxy chains,[39] combined with their fascinating electronic and photoconductive properties,[40] has stimulated investigations of these self-aggregating dye molecules for potential use in dye-sensitized organic solar cells. As became clear from earlier theoretical studies, Gouterman's four orbital model does not hold for porphyrazines and phthalocyanines as a result of the *meso*-tetraaza substitution of the aromatic macrocycle.[41] Differences up to 3 eV are calculated for the valence level energies between the first two MO's as a result of this substitution. These predictions have been confirmed by UPS measurements on free-base and metallo phthalocyanines.[42] Analogously to the approach discussed for porphyrins (*vide supra*) the IP's of a series of H$_2$Pc were investigated with both PM3 and AM1. The results of KT, OVGF and ΔSCF IP calculations are presented in Table 7.

Both KT and OVGF reproduce the large energy difference between the a$_u$ and b$_{3u}$ HOMO levels of H$_2$Pc. KT(AM1) computes the first IP at 7.15 eV, a discrepancy of 0.74 eV with the experimental number of 6.41 eV.[42] A much better result is obtained when the OVGF method is applied. OVGF(AM1) places IP$_1$ at 6.62 eV, which is a difference of 0.21 eV with the experimental first IP. A discrepancy of 0.45 eV is observed between OVGF(AM1) and OVGF(PM3). It should also be noted that an increase in the active orbital window size

increases the accuracy of IP$_1$ by 0.18 eV, but a better agreement between the calculated and experimental second IP for H$_2$Pc is obtained when the default setting of 20 HOMO's–20 LUMO's is used. The photoelectron spectrum of H$_2$Pc exhibits a broad ionization peak centered around 8.75 eV, which is probably the result of multiple ionizations and should therefore be interpreted as an average value. With ΔSCF IP(AM1) the lowest IP was calculated at 6.57 eV, in excellent agreement with the experimental value of 6.41 eV.

Substitution of the core-protons of free-base phthalocyanine by a zinc atom hardly affects the first IP. As is already observed from computations on H$_2$Pc, PM3 has major difficulties in computing the first IP of ZnPc. KT(PM3) computes IP$_1$ of ZnPc at 7.37 eV, a difference of 1 eV with the experimental value of 6.37 eV for ZnPc (see Table 8).[42] OGVF(PM3) improves on KT, IP$_1$ = 6.86 eV, but still a discrepancy of 0.49 eV with the literature value is observed, and with ΔSCF IP(PM3), IP$_1$ = 6.90 eV, no improvement is observed. AM1 yields significantly better data for this compound, which are with OVGF and ΔSCF IP both in fact well within experimental uncertainty. KT(AM1) computes IP$_1$ = 6.87 eV, which is a difference of 0.50 eV with the experimental first IP. Both OVGF(AM1) and ΔSCF IP(AM1) perform in this case superbly, and, respectively, predict the IP$_1$ at 6.46 and 6.39 eV. A distinct effect of metal insertion on the IP's is the increased resolution of the lower-lying MO's, which allows for a direct comparison of the higher experimental IP's of PcZn with the calculated data. These results are also presented in Table 8. Both AM1 and PM3 predict IP$_2$–IP$_4$ with approximately the same accuracy, and both agree well with the reported second, third and fourth IP of PcZn.[42] In contrast with the porphyrins, an increase of the active orbital window from the default value of 20 HOMO's–20 LUMO's to 60 HOMO's–60 LUMO's does not only improve the accuracy of the lowest IP, but unfortunately also yields an underestimation of the higher IP's. For free-base phthalocyanine this effect can not be addressed accurately, as there the higher IP's are not well resolved experimentally. In general, both OVGF(AM1) and ΔSCF IP(AM1) yield very good results with an active orbital window of 60 HOMO's–60 LUMO's, but no general statement on the effects of window size increases on the higher IP's can be made.

Conclusions

Six computational methods are benchmarked against *all* available ultraviolet photoelectron spectral (UPS) data on the vertical IP's of free-base and zinc porphyrins and phthalocyanines: Koopman's Theorem (KT), outer valence Green's function methods (OVGF), and explicit computation of the energy of both the neutral species and the radical cation (ΔSCF); all three methods in combination with both PM3 and AM1 parameterizations. In all cases studied both OVGF(AM1) and ΔSCF(AM1) reproduce the IP's, as determined by UPS, significantly more accurately than KT(AM1), and are for this purpose generally preferable over the analogous PM3 computations. The average error for the lowest IP's is for both OVGF(AM1) and ΔSCF(AM1) only *ca.* 40% of that computed with KT, and amounts to 0.33 and 0.35 eV, respectively. Although numerically very close for the lowest IP's studied in this work, OVGF-(AM1) has the advantage over ΔSCF(AM1) that information on higher IP's is also computed without extra effort or computation time. These methods allow for a significantly better correlation of computed ionization potentials with experimental data, which are frequently used to predict the properties of large aromatic compounds involved in electron-transfer processes.[43] The small average error, in combination with the small largest error found, make it possible to make fast predictions of the IP of extended aromatic compounds of which no experimental UPS or redox data exists. Such investigations of tetrapyrroles in order to analyze the influence of different heteroatoms directly attached to the macrocycle are in fact currently performed in our laboratories, and the results thereof will be reported in the near future.

Inclusion of higher order terms in the OVGF treatment (third order truncation or full expression of the self-energy part) does not affect the computed IP's. Extension of the number of active orbitals in the OVGF technique from 20 HOMO's–20 LUMO's to 60 HOMO's–60 LUMO's results in a systematic improvement of the calculated first IP's with only modest extra computational costs (longest OVGF computation in this paper: 610 seconds for OVGF(AM1) on TPPZn), and thus is the recommended active orbital window for tetrapyrroles. In agreement with the experimental data, zinc porphyrins and zinc phthalocyanines are computed to be better electron donors than their free-base analogues. Finally, conformational differences of the peripheral substituents are computed to have no significant effects on the valence IP's.

References

1 See for example: N. B. McKeown, *Phthalocyanine Materials: Synthesis, Structure and Function*, Cambridge University Press, Cambridge, 1998, ch. 6, pp. 126–139.

2 (*a*) C. F. van Nostrum, F. B. G. Benneker, N. Veldman, A. L. Spek, A.-J. Schouten and R. J. M. Nolte, *Recl. Trav. Chim. Pays-Bas*, 1994, **113**, 109; (*b*) C. F. van Nostrum, F. B. G. Benneker, H. Brussaard, H. Kooijman, N. Veldman, A. L. Spek, J. Schoonman, M. C. Feiters and R. J. M. Nolte, *Inorg. Chem.*, 1996, **35**, 959.

3 (*a*) J. T. Groves, M. Haushalter, M. Nakamura and B. J. Evans, *J. Am. Chem. Soc.*, 1981, **103**, 2884; (*b*) T. J. McMurry and J. T. Groves, in *Cytochrome P-450: Structure, Mechanism and Biochemistry*, ed. P. Ortiz de Montellano, Plenum Press, New York, 1986.

4 (*a*) J. M. Kroon, R. B. M. Koehorst, M. van Dijk, G. M. Sanders and E. J. R. Sudhölter, *J. Mater. Chem.*, 1997, **7**, 615; (*b*) D. P. Piet, H. Zuilhof and E. J. R. Sudhölter, unpublished work.

5 The adiabatic IP's of free-base porphyrin and free-base and zinc phthalocyanine were computed to be only 1–2 kcal mol⁻¹ lower than the vertical IP with the methods described in the Computational details section. Given the significant size of the π-system, this difference is expected to be small for all tetrapyrroles, and is thus near-constant as well. D. P. Piet, H. Zuilhof and E. J. R. Sudhölter, unpublished results.

6 (*a*) D. Schlettwein and N. R. Armstrong, *J. Phys. Chem.*, 1994, **98**, 11771; (*b*) S. V. Kudrevich and J. E. van Lier, *Can. J. Chem.*, 1996, **74**, 1718.

7 A. Koopman, *Physica*, 1933, **1**, 104.

8 T. Bally, in *Radical Ionic Systems*, eds. H. Lund and M. Shiotani, Kluwer Academic Publishers, Dordrecht, 1991, pp. 3–54.

9 E. Heilbronner, in *The Chemistry of Alkanes and Cycloalkanes*, ed. S. Patai, Wiley, New York, 1992, pp. 455–529.

10 (*a*) T. H. Dunning Jr. and P. J. Hay, in *Modern Theoretical Chemistry*, ed. H. F. Schaefer III, Plenum, New York, 1976, pp. 1–28; (*b*) T. H. Dunning Jr., *J. Chem. Phys.*, 1989, **90**, 1007; (*c*) A. D. McLean and G. S. Chandler, *J. Chem. Phys.*, 1980, **72**, 5639; (*d*) L. Åsbrink, C. Fridh and E. Lindholm, *Chem. Phys. Lett.*, 1977, **52**, 63.

11 D. P. Piet, H. Zuilhof and E. J. R. Sudhölter, unpublished results.

12 (*a*) P. G. Gassman, A. Ghosh and J. Almlöf, *J. Am. Chem. Soc.*, 1992, **114**, 9990; (*b*) A. Ghosh and J. Almlöf, *Chem. Phys. Lett.*, 1993, **213**, 519; (*c*) A. Ghosh, *J. Phys. Chem.*, 1994, **98**, 11004; (*d*) A. Ghosh, P. G. Gassman and J. Almlöf, *J. Am. Chem. Soc.*, 1994, **116**, 1932.

13 L. S. Cederbaum, *J. Phys. B*, 1975, **8**, 290.

14 (*a*) D. Danovich, V. Zakrzewski and E. Domnina, *J. Mol. Struct. (THEOCHEM)*, 1989, **188**, 159; (*b*) D. Danovich, Y. Apeloig and S. Shaik, *J. Chem. Soc., Perkin Trans. 2*, 1993, 321; (*c*) Y. Apeloig and D. Danovich, *Organometallics*, 1996, **15**, 350.

15 D. Danovich, in *Encyclopedia of Computational Chemistry, Vol. 2: Semiempirical methods*, ed. P v. R. Schleyer, Wiley, New York, 1998, pp. 1190–1202.

16 (*a*) L. S. Cederbaum and W. Domcke, *Adv. Chem. Phys.*, 1977, **36**, 206; (*b*) W. von Niessen, J. Schirmer and L S. Cederbaum, *Comput. Phys. Rep.*, 1984, **1**, 57.

17 J. V. Ortiz, V. G. Zakrzewski and O. Dolgounitcheva, in *Conceptual Trends in Quantum Chemistry*, ed. E. S. Kryachko, Kluwer, Dordrecht, 1997, vol. 3, pp. 465–517.

18 M. J. S. Dewar, E. G. Zoebish, E. F. Healy and J. P. P. Stewart, *J. Am. Chem. Soc.*, 1985, **107**, 3902.

19 J. P. P. Stewart, *J. Comput. Chem.*, 1989, **10**, 209.

20 MOPAC-93, J. P. P. Stewart and Fujitsu Limited, Tokyo, Japan, Fujitsu Limited, 1993.

21 GAUSSIAN94, Revision E.2, M. J. Frisch, G. W. Trucks, H. B. Schlegel, P. M. W. Gill, B. G. Johnson, M. A. Robb, J. R. Cheeseman, T. Keith, G. A. Petersson, J. A. Montgomery, K. Raghavachari, M. A. Al-Laham, V. G. Zakrzewski, J. V. Ortiz, J. B. Foresman, J. Cioslowski, B. B. Stefanov, A. Nanayakkara, M. Challacombe, C. Y. Peng, P. Y. Ayala, W. Chen, M. W. Wong, J. L. Andres, E. S. Replogle, R. Gomperts, R. L. Martin, D. J. Fox, J. S. Binkley, D. J. Defrees, J. Baker, J. P. Stewart, M. Head-Gordon, C. Gonzalez and J. A. Pople, Gaussian, Inc., Pittsburgh PA, 1995.

22 (*a*) A. C. Hurley, *Introduction to the electron theory of small molecules*, Academic Press, New York, 1976, pp. 242–253; (*b*) M. J. S. Dewar, *The molecular orbital theory of organic chemistry*, McGraw-Hill, New York, 1969, pp. 250–277; (*c*) In principle OVGF can be used for open-shell species when calculated with Dewar's half-electron method, but it can not be used on UHF wavefunctions within the present program realization in MOPAC. Use of OVGF on UHF-optimized geometries with single-point RHF wave-functions (OVGF on RHF/AM1//UHF/AM1) does not yield improved data over OVGF on RHF/AM1.

23 A. R. Leach, *Molecular Modelling, Principles and Applications*, Addison Wesley Longman Ltd., Harlow, 1996, pp. 25–130.

24 P. Depuis, R. Roberge and C. Sandorfy, *Chem. Phys. Lett.*, 1980, **75**, 434.

25 (*a*) M. Gouterman, G. Wagniere and L. C. Snyner, *J. Mol. Spectrosc.*, 1963, **11**, 108; (*b*) C. Weiss, H. Kobayashi and M. Gouterman, *J. Mol. Spectrosc.*, 1965, **16**, 415; (*c*) M. Gouterman, in *The Porphyrins*, ed. D. Dolphin, Academic Press, New York, 1978; Vol. III. Part A, Physical Chemistry.

26 S. Kitagawa, I. Morsihima, T. Yonezawa and N. Sato, *Inorg. Chem.*, 1979, **18**, 1345.

27 A. Ghosh, *J. Am. Chem. Soc.*, 1995, **117**, 4693.

28 (*a*) J.-H. Fuhrhop, K. M. Kadish and D. G. Davis, *J. Am. Chem. Soc.*, 1973, **95**, 5140; (*b*) J. G. Goll, K. T. Moore, A. Ghosh and M. J. Therien, *J. Am. Chem. Soc.*, 1996, **118**, 8344.

29 D. Wöhrle, L. Kreienhoop and D. Schlettwein, in *Phthalocyanines: Properties and Applications*, vol. 4, eds. C. C. Leznoff and A. B. P. Lever, VCH, New York, 1996, pp. 219–284.

30 S. C. Khandelwal and J. L. Roebber, *Chem. Phys. Lett.*, 1975, **34**, 355.

31 (*a*) T. D. Brennan, W. R. Scheidt and J. A. Shelnutt, *J. Am. Chem. Soc.*, 1988, **110**, 3919; (*b*) K. M. Barkigia, L. Chantranupong, K. M. Smith and J. Fajer, *J. Am. Chem. Soc.*, 1988, **110**, 7566; (*c*) K. M. Barkigia, M. D. Berber, M. D. J. Fajer, C. J. Medforth, M. W. Renner and K. M. Smith, *J. Am. Chem. Soc.*, 1990, **112**, 8851.

32 (*a*) M. J. Hamor, T. A. Hamor and J. L. Hoard, *J. Am. Chem. Soc.*,

1964, **86**, 1968; (*b*) S. J. Silvers and A. Tulinsky, *J. Am. Chem. Soc.*, 1967, **89**, 3331.

33 The AM1-minimization procedure converts the initial tetragonal and triclinic H$_2$TPP into a geometry which strongly resembles the tetragonal structure. In contrast, with PM3 optimization converts both structures into a geometry in which the porphyrin ring is planar and the phenyl groups are almost perpendicular to the macrocycle (almost D_{2h} symmetry). These findings will be discussed in a future comparative paper on semiempirical and DFT calculations of H$_2$TPP: F. J. Vergeldt, T. J. Schaafsma, D. P. Piet, E. J. R. Sudhölter and H. Zuilhof, manuscript in preparation.

34 K.–T. Lu, G. C. Eiden and J. C. Weisshaar, *J. Phys. Chem.*, 1992, **96**, 9742.

35 P. Cocolios and K. M. Kadish, *Israel J. Chem.*, 1985, **25**, 138.

36 K. Takahashi, T. Komura and H. Imanaga, *Bull. Chem. Soc. Jpn.*, 1989, **62**, 386.

37 C. H. Langford, S. Seto and B. R. Hollebone, *Inorg. Chim. Acta*, 1984, **90**, 221.

38 M. P. Byrn, C. J. Curtis, Y. Hsiou, S. I. Khan, P. A. Sawin, S. K. Tendick, A. Terzis and C. E. Strouse, *J. Am. Chem. Soc.*, 1993, **115**, 9480.

39 (*a*) J. F. van der Pol, E. Neeleman, J. W. Zwikker, R. J. M. Nolte and W. Drenth, *Liq. Cryst.*, 1989, **6**, 577; (*b*) P. G. Schouten, J. F. van der Pol, J. W. Zwikker, W. Drenth and S. J. Picken, *Mol. Cryst. Liq. Cryst.*, 1991, **195**, 291; (*c*) M. K. Engel, P. Bassoul, L. Bosio, H. Lehmann, M. Hanack and J. Simon, *Liq. Cryst.*, 1993, **15**, 709.

40 (*a*) N. Boden, R. J. Bushby and J. Clements, *J. Phys. Chem.*, 1993, **98**, 5920; (*b*) H. Ringsdorf and D. Haarer, *Nature*, 1994, **371**, 141; (*c*) P. Haish, G. Winter, W. Hanack, L. Lüer, H.-J. Egelhaaf and D. Oelkrug, *Adv. Mater.*, 1997, **9**, 316.

41 (*a*) A. Ghosh, P. G. Gassman and J. Almlöf, *J. Am. Chem. Soc.*, 1994, **116**, 1932; (*b*) D. Lamoen and M. Parrinello, *Chem. Phys. Lett.*, 1996, **248**, 309; (*c*) K. Toyota, J. Hasegawa and H. Nakatsuji, *Chem. Phys. Lett.*, 1996, **250**, 437.

42 J. Berkowitz, *J. Chem. Phys.*, 1979, **70**, 2819.

43 G. Schnurpfeil, A. K. Sobbi, W. Spiller, H. Kliesch and D. Wöhrle, *J. Porphyrins Phthalocyanines*, 1997, **1**, 159.